

A TIME DOMAIN INTEGRAL EQUATION SOLVER FOR SCATTERING FROM GENERAL CHIRAL OBJECTS

G.-P. Ye^{1, *} and Z.-H. Wu²

¹Network and Educational Technology Center, Zhanjiang Normal University, Zhanjiang, Guangdong 524048, China

²Argus Technologies (China) Ltd, Guangzhou 510730, China

Abstract—In this paper, transient electromagnetic scattering by general Chiral objects is investigated using time-domain integral equations with the Poggio, Miller, Chang, Harrington, Wu, and Tsai (PMCHWT) formulations. By introducing a pair of equivalent electric and magnetic currents, electromagnetic fields inside a homogeneous Chiral region can be represented by these sources over its boundary. The uncoupled equations are solved numerically by the Galerkin's method that involves separate spatial and temporal testing procedures. The scaled Laguerre functions are used as the temporal basis and testing functions. The use of the Laguerre functions completely removes the time variable from computation, and the results are stable even at late times. Numerical results are presented and compared with analytical results, and good agreements are observed.

1. INTRODUCTION

Bi-isotropic (BI) medium has emerged as one of the most challenging topics in electromagnetic research in terms of theoretical problems and potential applications in the last twenty years [1]. Chiral [2] and Tellegen [3] materials represent two subclass of BI medium, and most of the work has been studied on the interaction of the electromagnetic fields with chiral material. Chiral media were used in many applications involving antennas and arrays, antenna radomes, and waveguides [4–6]. The chiral object is optically active, and it means that the polarization plane of an electromagnetic (EM) wave is rotated when it is propagating through the chiral media. This can also

Received 23 April 2012, Accepted 31 May 2012, Scheduled 21 June 2012

* Corresponding author: Gu-Ping Ye (yegp@zhjnc.edu.cn).

be known as handedness. Object that have the property of handedness are said to be either right-handed or left-handed. Different from dielectric or conducting objects, chiral scatterers produce both co-polarized and cross-polarized scattered fields. Therefore, coating with chiral material is studied for reducing radar cross-section (RCS) of targets [7].

This paper is concerned with the numerical method to solve the EM scattering by general Chiral objects. Previously published solutions to the electromagnetic scattering by Chiral media were based on the method of moments (MoM) [8–10], multilevel Green's function interpolation method [9], plane wave decomposition [10], and the matrix Riccati equations [11]. While there have been many frequency-domain techniques reported, very little work has been done in the time-domain. The time-domain schemes available for Chiral media focus on the finite difference method, such as the finite-difference time-domain (FDTD) [12–14], the conformal FDTD [7], the BI-FDTD [15], and so on. The analysis examples were restricted to chiral spheres whose solutions can be analytically calculated with the modal expansion theory. Therefore, the applicability of the FDTD method still needs to be further verified for general Chiral objects.

Although the FDTD method has been the dominant tool for time domain simulations, the time-domain integral equation (TDIE) approach is preferable in some aspects especially for analysis of transient scattering by large-size bodies [16, 17]. The reason is that the TDIE method solves fewer unknowns using surface discretization and requires no artificial absorbing boundary condition (ABC). Recently, the marching-on in degree (MOD) method [18–21] using a set of scaled Laguerre polynomials as the temporal expansion and testing functions has been proposed. This method allows stable results to be obtained even at late times. To the best of our knowledge, this TDIE solver has not been used to deal with the scattering by Chiral media. Therefore, this work presents the first application of the TDIE method based on a MOD procedure for three-dimensional homogeneous Chiral objects.

In this paper, pairs of new sources are first defined and later introduced to formulate the far scattered fields by homogeneous dielectric objects in the time domain. Then the method is extended for constructing scattered fields inside and outside the Chiral medium. A field splitting scheme [1] is employed to simplify the expression of the EM fields inside the bodies. In order to achieve stable solutions, the Poggio, Miller, Chang, Harrington, Wu, and Tsai (PMCHWT) formulations [19–21] are used to construct the surface integral equations. After enforcing boundary conditions, a series of coupled integral equations are established and solved numerically by the MoM [22], involving separate spatial and temporal testing

procedures. The Rao-Wilton-Glisson (RWG) functions [23] are used as the spatial expansion and testing functions, and the weighted Laguerre functions are used as the temporal expansion and testing functions. The use of the Laguerre functions completely removes the time variable from computation, and the matrix equation is solved recursively using a MOD procedure. To validate the accuracy of the proposed TDIE method, the scattering of Chiral objects is analyzed, and the transient currents, far scattered fields and bistatic radar cross-sections are presented and compared.

2. THEORY AND EQUATIONS

2.1. Equivalent Sources for Homogeneous Dielectric Bodies

Consider a homogeneous dielectric body with a permittivity of ε_2 and a permeability of μ_2 in an infinite homogeneous medium with a permittivity of ε_1 and a permeability of μ_1 . A pair of new sources $\mathbf{e}(\mathbf{r}, t)$ and $\mathbf{h}(\mathbf{r}, t)$ on the surface S of the dielectric body are defined by

$$\mathbf{J}(\mathbf{r}, t) = \frac{\partial}{\partial t} \mathbf{e}(\mathbf{r}, t) \quad (1)$$

$$\mathbf{M}(\mathbf{r}, t) = \frac{\partial}{\partial t} \mathbf{h}(\mathbf{r}, t) \quad (2)$$

where $\mathbf{J}(\mathbf{r}, t)$ and $\mathbf{M}(\mathbf{r}, t)$ are the equivalent electric and magnetic surface currents.

The electric and magnetic fields \mathbf{E}^s and \mathbf{H}^s produced by electric and magnetic surface currents \mathbf{J} and \mathbf{M} , radiating into an unbounded space characterized by ε_1 and μ_1 are given by

$$\mathbf{E}^s = -\frac{\partial \mathbf{A}(\mathbf{r}, t)}{\partial t} - \nabla \Phi(\mathbf{r}, t) - \frac{1}{\varepsilon_1} \nabla \times \mathbf{F}(\mathbf{r}, t) \quad (3)$$

$$\mathbf{H}^s = -\frac{\partial \mathbf{F}(\mathbf{r}, t)}{\partial t} - \nabla \Psi(\mathbf{r}, t) + \frac{1}{\mu_1} \nabla \times \mathbf{A}(\mathbf{r}, t) \quad (4)$$

where \mathbf{A} and \mathbf{F} are the magnetic and electric vector potentials, respectively, and Φ and Ψ are the electric and magnetic scalar potentials given by

$$\mathbf{A}(\mathbf{r}, t) = \frac{\mu_1}{4\pi} \int_S \frac{\mathbf{J}(\mathbf{r}', \tau)}{R} dS' \quad (5)$$

$$\mathbf{F}(\mathbf{r}, t) = \frac{\varepsilon_1}{4\pi} \int_S \frac{\mathbf{M}(\mathbf{r}', \tau)}{R} dS' \quad (6)$$

$$\Phi(\mathbf{r}, t) = \frac{1}{4\pi\epsilon_1} \int_S \frac{q_e(\mathbf{r}', \tau)}{R} dS' \quad (7)$$

$$\Psi(\mathbf{r}, t) = \frac{1}{4\pi\mu_1} \int_S \frac{q_m(\mathbf{r}', \tau)}{R} dS' \quad (8)$$

where $R = |\mathbf{r} - \mathbf{r}'|$ represents the distance between the observation point \mathbf{r} ; the source point \mathbf{r}' , $\tau = t - R/c_1$ is the retarded time; $c_1 = 1/\sqrt{\epsilon_1\mu_1}$ is the velocity of the propagation of EM wave in space. The electric surface charge density q_e and magnetic surface charge density q_m are related to the electric current density \mathbf{J} and magnetic current density \mathbf{M} , respectively, by the equation of continuity

$$\nabla \cdot \mathbf{J}(\mathbf{r}, t) = -\frac{\partial}{\partial t} q_e(\mathbf{r}, t) \quad (9)$$

$$\nabla \cdot \mathbf{M}(\mathbf{r}, t) = -\frac{\partial}{\partial t} q_m(\mathbf{r}, t) \quad (10)$$

A pair of new sources $\mathbf{e}(\mathbf{r}, t)$ and $\mathbf{h}(\mathbf{r}, t)$ are defined in (1) and (2), so the charge density will be

$$q_e(\mathbf{r}, t) = -\nabla \cdot \mathbf{e}(\mathbf{r}, t) \quad (11)$$

$$q_m(\mathbf{r}, t) = -\nabla \cdot \mathbf{h}(\mathbf{r}, t) \quad (12)$$

Equations (5)–(8) will be changed as

$$\mathbf{A}(\mathbf{r}, t) = \frac{\mu_1}{4\pi} \int_S \frac{1}{R} \frac{\partial}{\partial t} \mathbf{e}(\mathbf{r}', \tau) dS' \quad (13)$$

$$\mathbf{F}(\mathbf{r}, t) = \frac{\epsilon_1}{4\pi} \int_S \frac{1}{R} \frac{\partial}{\partial t} \mathbf{h}(\mathbf{r}', \tau) dS' \quad (14)$$

$$\Phi(\mathbf{r}, t) = -\frac{1}{4\pi\epsilon_1} \int_S \frac{1}{R} \nabla \cdot \mathbf{e}(\mathbf{r}', \tau) dS' \quad (15)$$

$$\Psi(\mathbf{r}, t) = -\frac{1}{4\pi\mu_1} \int_S \frac{1}{R} \nabla \cdot \mathbf{h}(\mathbf{r}', \tau) dS' \quad (16)$$

Substitute Equations (13)–(16) to (3) and (4), respectively,

$$\begin{aligned} \mathbf{E}^s &= -\mu_1 \int_S \frac{1}{4\pi R} \frac{\partial^2 \mathbf{e}(\mathbf{r}, \tau)}{\partial t^2} dS' + \frac{\nabla}{\epsilon_1} \int_S \frac{\nabla \cdot \mathbf{e}(\mathbf{r}, \tau)}{4\pi R} dS' \\ &\quad - 0.5\hat{n} \times \frac{\partial \mathbf{h}(\mathbf{r}, t)}{\partial t} - \int_{S_0} \nabla \times \frac{1}{4\pi R} \frac{\partial \mathbf{h}(\mathbf{r}, \tau)}{\partial t} dS' \end{aligned} \quad (17)$$

$$\begin{aligned} \mathbf{H}^s = & -\varepsilon_1 \int_S \frac{1}{4\pi R} \frac{\partial^2 \mathbf{h}(\mathbf{r}, \tau)}{\partial t^2} dS' + \frac{\nabla}{\mu_1} \int_S \frac{\nabla \cdot \mathbf{h}(\mathbf{r}, \tau)}{4\pi R} dS' \\ & + 0.5 \hat{n} \times \frac{\partial \mathbf{e}(\mathbf{r}, t)}{\partial t} + \int_{S_0} \nabla \times \frac{1}{4\pi R} \frac{\partial \mathbf{e}(\mathbf{r}, \tau)}{\partial t} dS' \end{aligned} \quad (18)$$

where S_0 denotes the surface with the singularity at $\mathbf{r} = \mathbf{r}'$ removed from the surface S . We define two integro-differential operators L and K as follows,

$$L(\mathbf{X}) = \mu_1 \int_S \frac{\partial^2 \mathbf{X}(\mathbf{r}', \tau)}{\partial t^2} \frac{1}{4\pi R} dS' - \frac{\nabla}{\varepsilon_1} \int_S \frac{\nabla \cdot \mathbf{X}(\mathbf{r}', \tau)}{4\pi R} dS' \quad (19)$$

$$K(\mathbf{X}) = \frac{1}{2} \hat{n} \times \frac{\partial}{\partial t} \mathbf{X}(\mathbf{r}, t) + \int_{S_0} \nabla \times \left[\frac{\partial \mathbf{X}(\mathbf{r}', \tau)}{\partial t} \frac{1}{4\pi R} \right] dS' \quad (20)$$

Then, the total scattered electric and magnetic fields will be written as

$$\mathbf{E}^s(\mathbf{e}, \mathbf{h}) = -L(\mathbf{e}) - K(\mathbf{h}). \quad (21)$$

$$\mathbf{H}^s(\mathbf{e}, \mathbf{h}) = K(\mathbf{e}) - L(\mathbf{h}) / \eta_1^2. \quad (22)$$

It is noted that here we introduce a pair of new sources $\mathbf{e}(\mathbf{r}, t)$ and $\mathbf{h}(\mathbf{r}, t)$ instead of using conventional equivalent electrical current $\mathbf{J}(\mathbf{r}, t)$ and magnetic current $\mathbf{M}(\mathbf{r}, t)$ to construct the far-scattered fields. Such that, a time-integral term will disappear, and we can easily handle the time derivative of the electric and magnetic vector potentials.

2.2. Integral Equations for Scattering of Chiral Medium

Consider a homogenous Chiral body with a permittivity ε_2 and a permeability μ_2 in an infinite homogenous medium with a permittivity ε_1 and a permeability μ_1 . The expression of electric and magnetic fields inside the Chiral region are relatively complex because of the introduction of constitutive relations, namely

$$\mathbf{D} = \varepsilon_2 \mathbf{E} - j \kappa_r \sqrt{\varepsilon_2 \mu_2} \mathbf{H}. \quad (23)$$

$$\mathbf{B} = j \kappa_r \sqrt{\varepsilon_2 \mu_2} \mathbf{E} + \mu_2 \mathbf{H}. \quad (24)$$

where κ_r is the Pasteur parameter [1], and ε_2 and μ_2 are the permittivity and permeability of the Chiral medium. For a lossy material, these parameters are complex numbers. It is noticed that the above relations reduce to a conventional isotropic medium when κ_r is equal to zero.

These relations are frequency-domain expressions, which implicitly assume time-harmonic excitation in the $e^{j\omega t}$ convention. The time-domain expressions of the constitutive relations are given as follows [24],

$$\mathbf{D} = \varepsilon_2 \mathbf{E} - \chi_{CT} \frac{\partial \mathbf{H}}{\partial t} \quad (25)$$

$$\mathbf{B} = \mu_2 \mathbf{H} + \chi_{CT} \frac{\partial \mathbf{E}}{\partial t} \quad (26)$$

where

$$\chi_{CT} = \kappa_r \sqrt{\varepsilon_2 \mu_2} / \omega \quad (27)$$

The equivalent electric and magnetic sources on the surface of the BI media are denoted as $\mathbf{e}_b(\mathbf{r}, t)$ and $\mathbf{h}_b(\mathbf{r}, t)$, respectively, and surface currents are denoted as $\mathbf{J}_b(\mathbf{r}, t)$ and $\mathbf{M}_b(\mathbf{r}, t)$, respectively. The currents $\mathbf{J}_b(\mathbf{r}, t)$ and $\mathbf{M}_b(\mathbf{r}, t)$ can be expressed with these sources $\mathbf{e}_b(\mathbf{r}, t)$ and $\mathbf{h}_b(\mathbf{r}, t)$ as

$$\mathbf{J}_b(\mathbf{r}, t) = \frac{\partial}{\partial t} \mathbf{e}_b(\mathbf{r}, t) \quad (28)$$

$$\mathbf{M}_b(\mathbf{r}, t) = \frac{\partial}{\partial t} \mathbf{h}_b(\mathbf{r}, t) \quad (29)$$

The scattered fields \mathbf{E}_e^s and \mathbf{H}_e^s outside the Chiral media produced by the sources \mathbf{e}_b and \mathbf{h}_b is written as

$$\mathbf{E}_e^s(\mathbf{e}_b, \mathbf{h}_b) = -L(\mathbf{e}_b) - K(\mathbf{h}_b) \quad (30)$$

$$\mathbf{H}_e^s(\mathbf{e}_b, \mathbf{h}_b) = K(\mathbf{e}_b) - L(\mathbf{h}_b) / \eta_1^2 \quad (31)$$

To represent the fields inside the Chiral region, a field splitting scheme [1] is applied. Both the electric and magnetic fields \mathbf{E}_b^s and \mathbf{H}_b^s in the homogeneous Chiral medium are divided into the right- and left-circularly polarized wavefields. The right-polarized fields are denoted by “+” subscript, while the left-polarized components are denoted by “-” subscript. Therefore, we can write

$$\mathbf{E}_b^s = \mathbf{E}_{b+}^s + \mathbf{E}_{b-}^s \quad (32)$$

$$\mathbf{H}_b^s = \mathbf{H}_{b+}^s + \mathbf{H}_{b-}^s \quad (33)$$

The wavefields \mathbf{E}_{b+}^s (\mathbf{H}_{b+}^s) and \mathbf{E}_{b-}^s (\mathbf{H}_{b-}^s) are independent and uncoupled in the homogeneous Chiral medium. They are related to respective medium characterized by $\varepsilon_+(\varepsilon_-)$, $\mu_+(\mu_-)$, and $\eta_+(\eta_-)$, which are defined by

$$\varepsilon_{\pm} = \varepsilon_2(1 \pm \kappa_r) \quad (34)$$

$$\mu_{\pm} = \mu_2(1 \pm \kappa_r) \quad (35)$$

$$\eta_{\pm} = \sqrt{\mu_2 / \varepsilon_2} = \eta_2 \quad (36)$$

Since two wavefields are independently governed by Maxwell's equations, $\mathbf{E}_{b\pm}^s(\mathbf{H}_{b\pm}^s)$ and $\mathbf{E}_b^s(\mathbf{H}_b^s)$ can be expressed by

$$\mathbf{E}_{b\pm}^s = -L_{\pm}(\mathbf{e}_{b\pm}) - K_{\pm}(\mathbf{h}_{b\pm}) \quad (37)$$

$$\mathbf{H}_{b\pm}^s = K_{\pm}(\mathbf{e}_{b\pm}) - L_{\pm}(\mathbf{h}_{b\pm})/\eta_{\pm}^2 \quad (38)$$

where the integro-differential operators L_{\pm} and K_{\pm} are defined as

$$L_{\pm}(\mathbf{X}) = \mu_{\pm} \int_S \frac{\partial^2 \mathbf{X}(\mathbf{r}', \tau)}{\partial t^2} \frac{1}{4\pi R} dS' - \frac{\nabla}{\varepsilon_{\pm}} \int_S \frac{\nabla \cdot \mathbf{X}(\mathbf{r}', \tau)}{4\pi R} dS' \quad (39)$$

$$K_{\pm}(\mathbf{X}) = \int_{S_0} \nabla \times \left[\frac{\partial \mathbf{X}(\mathbf{r}', \tau)}{\partial t} \frac{1}{4\pi R} \right] dS' - \frac{1}{2} \hat{n} \times \frac{\partial}{\partial t} \mathbf{X}(\mathbf{r}, t) \quad (40)$$

As can be seen, the expressions of the scattered wavefields $\mathbf{E}_{b\pm}^s(\mathbf{H}_{b\pm}^s)$ and $\mathbf{E}_b^s(\mathbf{H}_b^s)$ in the media induced by $\mathbf{e}_{b+}(\mathbf{h}_{b+})$ and $\mathbf{e}_{b-}(\mathbf{h}_{b-})$ are similar to those of free space except that the material parameters are different. Here the relations of $(\mathbf{e}_b, \mathbf{h}_b)$ and $(\mathbf{e}_{b+}(\mathbf{h}_{b+}), \mathbf{e}_{b-}(\mathbf{h}_{b-}))$ can be obtained from Maxwell's equations [21],

$$-\mathbf{e}_{b\pm} = \frac{1}{2} \left(\mathbf{e}_b \mp \frac{j}{\eta_2} \mathbf{h}_b \right). \quad (41)$$

$$-\mathbf{h}_{b\pm} = \frac{1}{2} (\mathbf{h}_b \pm j\eta_2 \mathbf{e}_b) \quad (42)$$

To determine the unknown sources \mathbf{e}_b and \mathbf{h}_b , the boundary condition needs to be enforced on the Chiral scatterer surface.

$$-\mathbf{E}^{\text{in}}(\mathbf{r}, t)|_{\text{tan}} - \mathbf{E}_e^s(\mathbf{e}_b, \mathbf{h}_b)|_{\text{tan}} + \sum_{\pm} \mathbf{E}_{b\pm}^s(\mathbf{e}_{b\pm}, \mathbf{h}_{b\pm})|_{\text{tan}} = 0 \quad (43)$$

$$-\mathbf{H}^{\text{in}}(\mathbf{r}, t)|_{\text{tan}} - \mathbf{H}_e^s(\mathbf{e}_b, \mathbf{h}_b)|_{\text{tan}} + \sum_{\pm} \mathbf{H}_{b\pm}^s(\mathbf{e}_{b\pm}, \mathbf{h}_{b\pm})|_{\text{tan}} = 0 \quad (44)$$

where subscript "tan" defines tangential components, \mathbf{E}^{in} and \mathbf{H}^{in} are the incident electric and magnetic fields.

2.3. Basis Functions and Testing Scheme

MoM is adopted to solve the Equations (43) and (44). For the numerical implementation, the equivalent electric and magnetic currents $\mathbf{e}_b(\mathbf{r}, t)$ and $\mathbf{h}_b(\mathbf{r}, t)$ are represented in terms of RWG functions by

$$\mathbf{e}_b(\mathbf{r}, t) = \sum_{n=1}^N \sum_{j=0}^{\infty} e_{bn,j} \phi_j(st) \mathbf{f}_n(\mathbf{r}) \quad (45)$$

$$\mathbf{h}_b(\mathbf{r}, t) = \sum_{n=1}^N \sum_{j=0}^{\infty} h_{bn,j} \phi_j(st) \mathbf{f}_n(\mathbf{r}) \quad (46)$$

where N is the number of the inner edges; $e_{bn,j}$ and $h_{bn,j}$ are the unknown coefficients; $\phi_j(st) = e^{-st/2}L_j(st)$ is the causal temporal basis function. $\mathbf{f}_n(\mathbf{r})$ represents the RWG function, and $L_j(st)$ is the Laguerre function [25] of degree j with scaling factor s .

Substituting (45) to (19) and (20) respectively, we obtained

$$L(\mathbf{e}_b) = \mu_0 s^2 \sum_{n=1}^N \sum_{j=0}^{\infty} \int_{S_0} \frac{1}{4\pi R} \left(0.25e_{bn,j} + \sum_{k=0}^{j-1} (j-k)e_{bn,k} \right) \phi_j(s\tau) \mathbf{f}_n(\mathbf{r}) dS' \\ - \frac{1}{\varepsilon_0} \sum_{n=1}^N \sum_{j=0}^{\infty} e_{bn,j} \nabla \int_S [\nabla \cdot \mathbf{f}_n(\mathbf{r})] \frac{\phi_j(s\tau)}{4\pi R} dS' \quad (47)$$

$$K(\mathbf{e}_b) = 0.5\hat{n} \times s \sum_{n=1}^N \sum_{j=0}^{\infty} \left(0.5e_{bn,j} + \sum_{k=0}^{j-1} e_{bn,k} \right) \phi_j(s\tau) \mathbf{f}_n(\mathbf{r}) \\ + \frac{s^2}{c_0} \sum_{n=1}^N \sum_{j=0}^{\infty} \int_{S_0} \left(0.25e_{bn,j} + \sum_{k=0}^{j-1} (j-k)e_{bn,k} \right) \phi_j(s\tau) \mathbf{f}_n(\mathbf{r}) \times \hat{R} / R dS' \\ + s \sum_{n=1}^N \sum_{j=0}^{\infty} \int_{S_0} \left(0.5e_{bn,j} + \sum_{k=0}^{j-1} e_{bn,k} \right) \phi_j(s\tau) \mathbf{f}_n(\mathbf{r}) \times \hat{R} / R^2 dS' \quad (48)$$

Since $L(\mathbf{h}_b)$ is identical as $L(\mathbf{e}_b)$ in Equation (47), and $K(\mathbf{h}_b)$ is identical as $K(\mathbf{e}_b)$ in (48), the formulations are omitted here.

In computing the spatial integrals in (47) and (48), the functions dependent on the following variable do not change appreciably within a given triangular patch so that

$$\tau_v = t - \frac{R}{c_v}, \quad \tau_{mn,v}^{pq} = t - \frac{R_{mn}^{pq}}{c_v}, \quad R_{mn}^{pq} = |\mathbf{r}_m^{cp} - \mathbf{r}_n^{cq}| \quad (49)$$

where p , q , and v can be either $+$ or $-$, and \mathbf{r}_m^{cp} and \mathbf{r}_n^{cq} are the position vectors of the center points in triangle pair T_m^{\pm} .

Through the Galerkin's method [22], we take a spatial and a temporal testing with $\mathbf{f}_m(\mathbf{r})$ ($m = 1, 2, \dots, N$) and $\phi_i(st)$ ($i = 0, 1, 2, \dots, M$) separately to the Equation (43), where M is the maximum degree of the Laguerre functions to be evaluated from the time-bandwidth product of the waveform. It is noted that the testing functions are exactly the same as the basis functions. The equation below is obtained

$$\langle \phi_i(st), \langle \mathbf{f}_m(\mathbf{r}), L(\mathbf{e}_b) \rangle \rangle + \langle \phi_i(st), \langle \mathbf{f}_m(\mathbf{r}), K(\mathbf{h}_b) \rangle \rangle \\ - \sum_{\pm} \langle \phi_i(st), \langle \mathbf{f}_m(\mathbf{r}), L_{\pm}(\mathbf{e}_{b_{\pm}}) \rangle \rangle - \sum_{\pm} \langle \phi_i(st), \langle \mathbf{f}_m(\mathbf{r}), K_{\pm}(\mathbf{h}_{b_{\pm}}) \rangle \rangle \\ = \langle \phi_i(st), \langle \mathbf{f}_m(\mathbf{r}), \mathbf{E}^{\text{in}} \rangle \rangle \quad (50)$$

First, we consider the testing of the integro-differential operator L with the electric source \mathbf{e}_b . With reference to [18], the testing formulation can be written as

$$\begin{aligned} \langle \phi_i(st), \langle \mathbf{f}_m(\mathbf{r}), L(\mathbf{e}_b(\mathbf{r}, t)) \rangle \rangle &= \frac{1}{\varepsilon_0} \sum_{n=1}^N \sum_{p,q} \sum_{j=0}^i e_{bn,j} I_{ij}(s\tau_{mn}^{pq}) b_{mn,1}^{pq} \\ &+ \mu_0 s^2 \sum_{n=1}^N \sum_{p,q} \sum_{j=0}^i \left(0.25 e_{bn,j} + \sum_{k=0}^{j-1} (j-k) e_{bn,k} \right) I_{ij}(s\tau_{mn}^{pq}) a_{mn,1}^{pq} \end{aligned} \quad (51)$$

where inner integral $\langle \mathbf{f}_m(\mathbf{r}) \rangle$ denotes a spatial testing which is defined by multiplying the function $\mathbf{f}_m(\mathbf{r})$ and integrating in the triangle pairs T_m^\pm on the Chiral object surface, and $\langle \phi_i(st) \rangle$, represents a temporal testing, which is done by multiplying the function $\phi_i(st)$ and integrating from zero to infinity. The temporal testing can be simplified as

$$I_{ij}(s\tau_{mn}^{pq}) = \begin{cases} e^{-s\tau_{mn}^{pq}/2} [L_{i-j}(s\tau_{mn}^{pq}) - L_{i-j-1}(s\tau_{mn}^{pq})] & j \leq i \\ 0 & j > i \end{cases} \quad (52)$$

and the expression of the spatial integrals $a_{mn,1}^{pq}$ and $b_{mn,1}^{pq}$ between triangles on surface of the Chiral scatterer are given by

$$a_{mn,1}^{pq} = \int_S \int_{S'} \mathbf{f}_m^p(\mathbf{r}) \cdot \mathbf{f}_n^q(\mathbf{r}') / (4\pi R) dS' dS \quad (53)$$

$$b_{mn,1}^{pq} = \int_S \nabla \cdot \mathbf{f}_m^p(\mathbf{r}) \int_{S'} \nabla \cdot \mathbf{f}_n^q(\mathbf{r}') / (4\pi R) dS' dS \quad (54)$$

Then we consider the second testing term of the left-hand side in (50), and it becomes

$$\begin{aligned} \langle \phi_i(st), \langle \mathbf{f}_m(\mathbf{r}), K(\mathbf{h}_b(\mathbf{r}, t)) \rangle \rangle &= s \sum_{n=1}^N \sum_{p,q} \sum_{j=0}^i \left(0.5 h_{bn,j} + \sum_{k=0}^{j-1} h_{bn,k} \right) I_{ij}(s\tau_{mn}^{pq}) \\ d_{mn,12}^{pq} + s^2/c_0 \sum_{n=1}^N \sum_{p,q} \sum_{j=0}^i \left(0.25 h_{bn,j} + \sum_{k=0}^{j-1} (j-k) h_{bn,k} \right) &I_{ij}(s\tau_{mn}^{pq}) d_{mn,11}^{pq} \end{aligned} \quad (55)$$

where the expression of the spatial integrals $d_{mn,11}^{pq}$ and $d_{mn,12}^{pq}$ between triangles on the surface of the Chiral object are given by

$$d_{mn,11}^{pq} = \int_S \int_{S'} \mathbf{f}_m^p(\mathbf{r}) \cdot \mathbf{f}_n^q(\mathbf{r}') \times \hat{R} / (4\pi R) dS' dS \quad (56)$$

$$d_{mn,12}^{pq} = \int_S \int_{S'} \mathbf{f}_m^p(\mathbf{r}) \cdot \mathbf{f}_n^q(\mathbf{r}') \times \hat{R} / (4\pi R^2) dS' dS \quad (57)$$

The integral in Equations (56) and (57) may be evaluated using the Gaussian quadrature integral scheme for unprimed and primed coordinates numerically [23]. Next the third and fourth term of the left-hand side of the equation (50) can be expressed in the same way when incorporating the relationship (41) and (42) into Equations (39) and (40).

Similarly, we take a spatial and a temporal testing with $\mathbf{f}_m(\mathbf{r})$ ($m = 1, 2, \dots, N$) and $\phi_i(st)$ ($i = 0, 1, 2, \dots, M$) to Equations (43) and (44), and all the testing procedures can be done easily.

After applying both spatial and temporal testing procedures to Equations (43) and (44), the $2N \times 2N$ matrix below is obtained after some mathematical manipulation,

$$\begin{bmatrix} [ZE_{mn}^E]_{N \times N} & [ZE_{mn}^H]_{N \times N} \\ [ZH_{mn}^E]_{N \times N} & [ZH_{mn}^H]_{N \times N} \end{bmatrix} \begin{bmatrix} [e_{bn,i}]_{N \times 1} \\ [h_{bn,i}]_{N \times 1} \end{bmatrix} = \begin{bmatrix} [\gamma_{m,i}^E]_{N \times 1} \\ [\gamma_{m,i}^H]_{N \times 1} \end{bmatrix} \quad (58)$$

To obtain the coefficients $e_{n,j}$ and $h_{n,j}$, we need to solve the matrix recursively on the degree of the Laguerre function. Particularly in the first step when $i = 0$, only system matrix elements ZE_{mn}^E , ZE_{mn}^H , ZH_{mn}^E , and ZH_{mn}^H are needed and the matrix LU decomposition can be stored for further use. At the i th step, we only have to compute $\gamma_{m,i}^E$ and $\gamma_{m,i}^H$ on the right side of the matrix, which are the sums of the previous solved coefficients $e_{n,j}$ and $h_{n,j}$. The detailed expressions of these elements are similar to those of Bi-isotropic scatterer given in chapter 4 of reference [21]. The complexities of this method are $O(12MN^2)$ for the filling procedure and $O(M^3N^2)$ for the iteration procedure. M is the maximum time degree of temporal testing function, and N is the number of the inner edges of the triangular mesh of the object surface.

3. RESULTS AND DISCUSSION

In this section, the numerical results for 3-D Chiral scatterer placed in free space will be presented to validate the previously described TDIE scheme. The scatterers are illuminated by a Gaussian plane wave as shown in Figure 1, in which the electric fields are given by

$$\mathbf{E}^i(\mathbf{r}, t) = 4\mathbf{E}_0 e^{-\gamma^2} / (\sqrt{\pi}T). \quad (59)$$

where $\gamma = (4/T)(ct - ct_0 - \mathbf{r} \cdot \hat{\mathbf{k}})$, $\hat{\mathbf{k}}$ is the unit vector in the direction of the wave propagation, T the pulse width, and ct_0 the time delay. In this work, the field is incident from $\varphi = 0^\circ$ and $\theta = 0^\circ$ with $\hat{\mathbf{k}} = \hat{\mathbf{z}}$, and $\mathbf{E}_0 = \hat{\mathbf{x}}$.

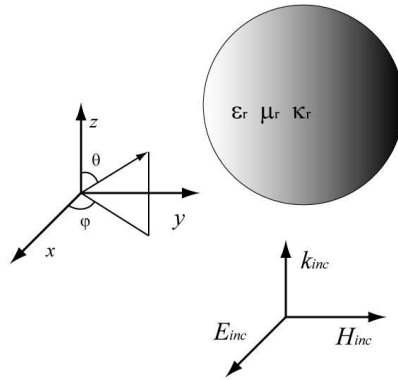


Figure 1. The 3-D Chiral sphere and coordinates illustrations.

The first example is the scattering from a dielectric sphere of radius 0.5 m centered at the origin. The sphere has a permittivity of $\epsilon_r = 4.0$ and a permeability of $\mu_r = 1.0$. FEKO [26] is used to mesh the sphere surface, which has a total of 616 patches and 924 edges. The Gaussian pulse of $T = 8 \text{ lm}$ and $ct_0 = 12 \text{ lm}$ is used in the numerical computation this time. The unit ‘lm’ denotes a light meter and represents the length of time taken by the electromagnetic wave to travel 1 m in free space. In the computation, we set $s = 1.0 \times 10^9$ and $M = 80$, which is sufficient to get accurate results. The exact solutions obtained using the Mie series are presented for comparison.

The choice of factor s and maximum temporal degree M is very crucial because these two parameters decide the amount of support given by the Laguerre functions in the time-domain response [27]. For dielectric bodies problems, the initial value of these parameters are set as $M = 2BT_f + 1$, and $s = 10f_{\max}$ [19], where B and T_f are the frequency bandwidth and time duration of the excitation signal, and f_{\max} is the maximum frequency.

Figure 2 depicts the computed backward scattered fields, while the forward scattered fields are shown in Figure 3. The Mie series are also presented for comparison [23]. We can see that both the backward and forward scattered fields are stable and in good agreement with the Mie series. As a special case, this example exhibits somewhat the accuracy of the proposed TDIE formula for Chiral media.

Then a chiral sphere with radius of 0.01 m is analyzed and the constitutive parameter is set as $\kappa_r = 0.15$. The Gaussian pulse of $T = 0.5 \text{ lm}$ and $ct_0 = 0.1 \text{ lm}$ is used in the numerical computation.

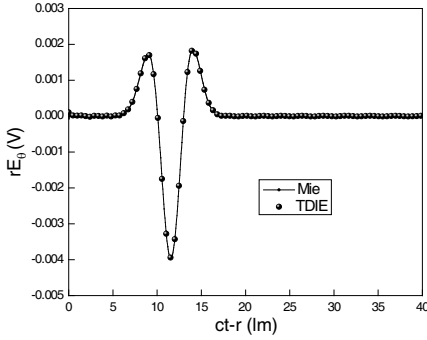


Figure 2. Backward scattered far-field from the dielectric sphere.

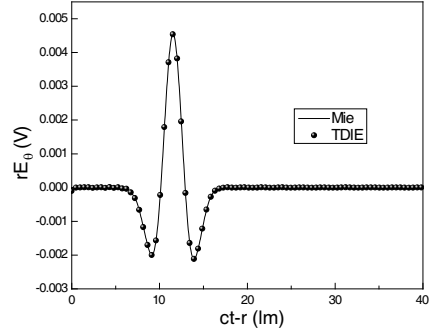


Figure 3. Forward scattered far-field from the dielectric sphere.

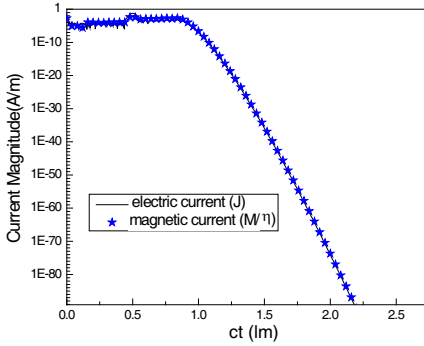


Figure 4. Transient currents at the point $(0.0096, 0.0022, 0.0005)$ on a 0.01 m radius chiral sphere (logarithm scale). The parameters of the sphere are $\varepsilon_r = 4.0$, $\mu_r = 1.0$, $\kappa_r = 0.15$.

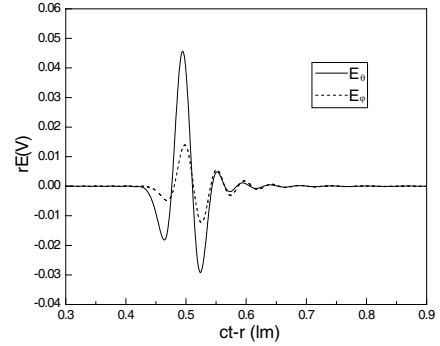


Figure 5. Normalized forward scattered fields of the chiral sphere. The sphere has a radius of 0.01 m, and other parameters are $\varepsilon_r = 4.0$, $\mu_r = 1.0$, $\kappa_r = 0.15$.

The maximum temporal degree $M = 110$ is used. The currents on one point of the sphere are shown in Figure 4 and stable results are observed at a very late time. The normalized forward transient response of the electric fields is plotted in Figure 5, and the φ -component of the scattered fields is observed. Figure 6 displays the forward co- and cross-polarized bistatic echo widths in a broad frequency band from 0 to 9 GHz. The analytical results [11] are also shown for comparison, and they agree well with the proposed TDIE solution. It is noticed

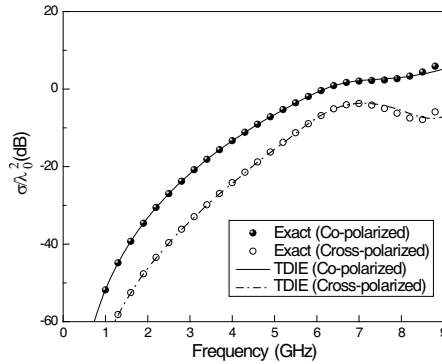


Figure 6. Forward co- and cross-polarized bistatic echo widths of the chiral sphere as a function of frequency. The sphere has a radius of 0.01 m, and other parameters are chosen with $\epsilon_r = 4.0$, $\mu_r = 1.0$, $\kappa_r = 0.15$.

that the exact and TDIE results seem to diverge in the frequencies higher than 9 GHz. The reason is that the incident Gaussian pulse of $T = 0.5$ ns and $ct_0 = 0.1$ ns used has a spectrum of 9 GHz, and the computed results higher than 9 GHz will not be correct.

We also make a comparison between the proposed TDIE method with the FDTD approach. The chiral sphere is chosen as the scatterer, which was computed using FDTD [14] as well as analytical method [11]. The sphere has a radius of 7.2 cm, and other parameters are chosen as $\epsilon_r = 4.0$, $\mu_r = 1.0$, and $\kappa_r = 0.25$. The sphere is meshed using 616 triangular patches, and the Gaussian pulse has a peak at 1.0 ns with width of 0.8 ns. The maximum temporal degree M is set as 120. The computed forward co- and cross-polarized radar cross-sections as a function of the elevation angles at 1 GHz are shown in Figure 7, and the accuracy of the TDIE method is approved by the FDTD method and analytical results.

4. EXTENSION TO THE DISPERSIVE CASE

Owing to the fact that the constitutive parameters are non-dispersive, the equations above-mentioned are set up for high idealized model. It is not very difficult for us to extend the proposed method for frequency dependent materials. The TDIE method based on the MOD procedure is one of the recursive convolution techniques that allow linear dispersion to be incorporated like FDTD [13, 14] formulation.

Considering the dispersive chiral media, the electric and magnetic fields are decomposed into the wavefields and the scattering problem

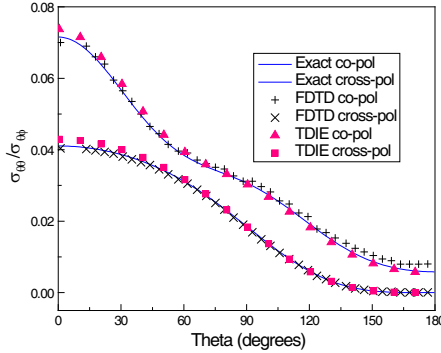


Figure 7. Computed forward co- and cross-polarized radar cross-sections of a 7.2 cm radius chiral sphere with comparison with FDTD method at frequency 1GHz. The parameters of the sphere are $\varepsilon_r = 4.0$, $\mu_r = 1.0$, and $\kappa_r = 0.25$.

is treated as the sum of two problems in associated isotropic media. After using the fields splitting scheming, the Equations (34)–(36) will become

$$\varepsilon_{\pm}(\omega) = \varepsilon_2(1 \pm \kappa_r(\omega)) \quad (60)$$

$$\mu_{\pm}(\omega) = \mu_2(1 \pm \kappa_r(\omega)) \quad (61)$$

$$\eta_{\pm} = \sqrt{\mu_2/\varepsilon_2}v_{\mp} = \eta_2 \quad (62)$$

where the frequency variation of the chirality term is expressed by the Condon model [1].

The fields inside the chiral media can be constructed using the integro-differential operators L_{\pm} and K_{\pm} . Different from non-dispersive formulations (39) and (40), these two operators will have an additional time-integral term. After applying boundary condition, the coupled integral equations can be obtained. For the testing procedure, the temporal integral Equation (52) will become a little complicated because of the additional time-integral term. This will be the further work in the near future.

5. CONCLUSION

The TDIE solver based on the MOD procedure is proposed to calculate the scattering of Chiral objects with arbitrary shape. The integral equations are solved with Galerkin's method, which involves separate spatial and temporal testing procedures. The RWG functions are used as the spatial expansion and testing functions. The weighted Laguerre

polynomials are used as the temporal expansion and testing functions. Numerical results are shown to agree well with the analytical results and FDTD method. In later work, this method will be extended for scattering problems of layered Chiral objects and antenna loaded Chiral materials.

REFERENCES

1. Lindell, I. V., A. H. Sihvola, S. A. Tretyakov, and A. J. Viitanen, *Electromagnetic Waves in Chiral and Bi-isotropic Media*, Artech House, Boston, MA, 1994.
2. Lindell, I. V., S. A. Tretyakov, and M. I. Oksanen, "Conductor-backed Tellegen slab as twist polarizer," *Electron. Lett.*, Vol. 28, No. 3, 281–282, Jan. 1992.
3. Tellegen, B. D. H., "The gyrator: A new electric network element," *Phillips Res. Rep.*, Vol. 3, 81, 1948.
4. Tretyakov, S. A. and A. A. Sochava, "Proposed composite material for nonreflecting shields and antenna radomes," *Electron Lett.*, Vol. 29, 1048–1049, Jun. 1993.
5. Engheta, N. and P. Pelet, "Reduction of surface waves in chirostrip antennas," *Electron Lett.*, Vol. 27, 5–7, Jan. 1991.
6. Pelet, P. and N. Engheta, "The theory of chirowaveguides," *IEEE Trans. on Antennas and Propagat.*, Vol. 38, 90–98, Jan. 1990.
7. Zheng, H. X., X. Q. Sheng, and E. K. N. Yung, "Computation of scattering from conducting bodies coated with chiral materials using conformal FDTD," *Journal of Electromagnetic Waves and Applications*, Vol. 18, No. 11, 1471–1484, 2004.
8. Kluskens, M. S., "Method of moments analysis of scattering by chiral media," Ph.D. Dissertation, Ohio State University, Columbus, OH, 1991.
9. Shi, Y. and C. H. Chan, "Solution to electromagnetic scattering by bi-isotropic media using multilevel Green's functions interpolation method," *Progress In Electromagnetic Research*, Vol. 97, 259–274, 2009.
10. Worasawate, D., "Electromagnetic scattering from an arbitrarily shaped three-dimensional chiral body," Ph.D. Dissertation, Syracuse University, Syracuse, NY, 2002.
11. Jaggard, D. L. and J. C. Liu, "The matrix Riccati equation for scattering from stratified chiral spheres," *IEEE Trans. on Antennas and Propagat.*, Vol. 47, No. 7, 1201–1207, Jul. 1999.
12. Garcia, S. G., I. V. Perez, R. G. Martin, et al., "Extension of

- berenger's PML for bi-isotropic media," *IEEE Microwave Guided Wave Lett.*, Vol. 8, No. 9, 297–299, 1998.
13. Demir, V., A. Z. Elsherbeni, and E. Arvas, "FDTD formulation for dispersive chiral media using the Z transform method," *IEEE Trans. on Antennas and Propogat.*, Vol. 53, No. 10, 3374–3384, Oct. 2005.
 14. Demir, V., "Electromagnetic scattering from three dimensional chiral objects using the FDTD method," Ph.D. Dissertation, Syracuse University, Jun. 2004.
 15. Semichaevsky, A., A. Akyurtlu, D. Kern, et al., "Novel BI-FDTD approach for the analysis of chiral cylinders and spheres," *IEEE Trans. on Antennas and Propagat.*, Vol. 54, No. 3, 925–932, Mar. 2006.
 16. Rao, S. M., *Time-domain Electromagnetics*, Academic Press, San Diego, 1999.
 17. Chen, Z. Z. and M. M. Ney, "The method of weighted residuals: A general approach to deriving time- and frequency-domain numerical methods," *IEEE Antennas Propagat. Mag.*, Vol. 51, No. 1, 51–70, Feb. 2009.
 18. Jung, B. H., T. K. Sarkar, Y. S. Chung, S. P. Magdalena, Z. Ji, S. Jang, and K. Kim, "Transient electromagnetic scattering from dielectric objects using the electric field integral equation with Laguerre polynomials as temporal basis functions," *IEEE Trans. on Antennas Propogat.*, Vol. 52, No. 9, 2329–2339, Sept. 2004.
 19. Jung, B. H., M. T. Yuan, T. K. Sarkar, et al., "Solving the time-domain magnetic field integral equation for dielectric bodies without the time variable through the use of entire domain Laguerre polynomials," *Electromagn.*, Vol. 24, No. 6, 385–408, Sept. 2004.
 20. Jung, B. H., T. K. Sarkar, and Y.-S. Chung, "Solution of time domain PMCHW formulation for transient electromagnetic scattering from arbitrarily shaped 3-D dielectric objects," *Progress In Electromagnetics Research*, Vol. 45, 291–312, 2004.
 21. Wu, Z. H., "Time domain integral equations for scattering and radiation by three-dimensional homogeneous Bi-isotropic objects with arbitrary shape," Ph.D. Dissertation, City University of Hong Kong, Hong Kong, Jul. 2010.
 22. Ney, M. M., "Method of moments as applied to electromagnetic problems," *IEEE Trans. on Microwave Theory and Techniques*, Vol. 33, No. 10, 972–980, Nov. 1985.
 23. Rao, S. M., "Electromagnetic scattering and radiation of

- arbitrarily shaped surfaces by triangular patch modeling,” Ph.D. Dissertation, University Mississippi, Aug. 1980.
24. Sihvola, A. H. and I. V. Lindell, “Bi-isotropic constitutive relations,” *Microwave Opt. Technol. Lett.*, Vol. 4, No. 8, 295–297, Jul. 1991.
 25. Gradshteyn, I. S. and I. M. Ryzhik, *Table of Integrals, Series and Products*, Academic, New York, 1980.
 26. FEKO electromagnetic simulation software, Available online: <http://www.feko.info>.
 27. Zhu, H., Z.-H. Wu, X.-Y. Zhang, and B.-J. Hu, “Time-domain integral equation solver for radiation from dipole loaded with general Bi-isotropic objects,” *Progress In Electromagnetics Research B*, Vol. 35, 349–367, 2011.